AGU PUBLICATIONS

Geophysical Research Letters

RESEARCH LETTER
10.1002/2016GL068335

Key Points:
- N_2 fixation decreases in response to atmospheric nitrogen deposition
- Denitrification increases in response to atmospheric nitrogen deposition
- Nitrogen cycle feedbacks stabilize marine nitrogen inventory and limit changes to productivity

Supporting Information:
- Supporting Information S1

Correspondence to:
C. J. Somes,
csomes@geomar.de

Citation:
Somes, C. J., A. Landolfi, W. Koeve, and A. Oschlies (2016), Limited impact of atmospheric nitrogen deposition on marine productivity due to biogeochemical feedbacks in a global ocean model, *Geophys. Res. Lett.*, *43*, 4500–4509, doi:10.1002/2016GL068335.

Received 27 OCT 2015
Accepted 15 APR 2016
Accepted article online 28 APR 2016
Published online 14 MAY 2016

Limited impact of atmospheric nitrogen deposition on marine productivity due to biogeochemical feedbacks in a global ocean model

Christopher J. Somes[1], Angela Landolfi[1], Wolfgang Koeve[1], and Andreas Oschlies[1]

[1]GEOMAR Helmholtz Centre for Ocean Research Kiel, Kiel, Germany

Abstract The impact of increasing anthropogenic atmospheric nitrogen deposition on marine biogeochemistry is uncertain. We performed simulations to quantify its effect on nitrogen cycling and marine productivity in a global 3-D ocean biogeochemistry model. Nitrogen fixation provides an efficient feedback by decreasing immediately to deposition, whereas water column denitrification increases more gradually in the slowly expanding oxygen deficient zones. Counterintuitively, nitrogen deposition near oxygen deficient zones causes a net loss of marine nitrogen due to the stoichiometry of denitrification. In our idealized atmospheric deposition simulations that only account for nitrogen cycle perturbations, these combined stabilizing feedbacks largely compensate deposition and suppress the increase in global marine productivity to $<2\%$, in contrast to a simulation that neglects nitrogen cycle feedbacks that predicts an increase of $>15\%$. Our study emphasizes including the dynamic response of nitrogen fixation and denitrification to atmospheric nitrogen deposition to predict future changes of the marine nitrogen cycle and productivity.

1. Introduction

Nitrogen is an essential element for life that limits marine productivity throughout much of the surface ocean. In the preindustrial ocean, bioavailable fixed nitrogen (fixed N) was predominantly supplied by N_2-fixing microorganisms (diazotrophs) and was removed by denitrification (including anammox) in oxygen deficient zones (ODZs, $O_2 < \sim 10\,\mathrm{mmol\ m^{-3}}$), where anaerobic respiration of organic matter occurs, in the water column and in sediments [*Gruber*, 2008]. Anthropogenic N emissions and subsequent deposition into the ocean are rapidly increasing [*Duce et al.*, 2008] and approaching estimates of N_2 fixation by diazotrophs [*Gruber*, 2008], which may alter the balance of marine fixed-N inventory and productivity in the future ocean. It is not yet understood how marine ecosystems will respond to increasing levels of atmospheric N deposition, but it has been suggested that atmospheric N deposition may relieve N limitation in the ocean and stimulate additional production [*Kim et al.*, 2014] that could help buffer rising atmospheric CO_2 by sequestering carbon in the ocean.

The dynamic global response of N_2 fixation, water column denitrification, and sedimentary denitrification to atmospheric N deposition has yet to be quantitatively understood. Since diazotrophs may have an ecological advantage in N-depleted waters, atmospheric N deposition has been suggested to reduce their ecological niche, as found in a global ocean biogeochemistry model [*Krishnamurthy et al.*, 2009]. However, no previous model studies have quantified the feedbacks of sedimentary denitrification, the largest fixed-N sink in the ocean, on the global fixed-N inventory, and marine productivity in response to N deposition.

Atmospheric N deposition to surface waters nearby ODZs and continental shelves has the potential to stimulate additional biological production, expanding ODZs and subsequent denitrification. Since denitrification consumes ~7 mol nitrate per mol organic nitrogen remineralized [*Richards*, 1965], organic matter produced from atmospheric N deposition that is respired anaerobically via denitrification in ODZs or shelf sediments may lead to a net loss in the fixed-N inventory [*Landolfi et al.*, 2013]. In this study, we use a global 3-D ocean biogeochemical model that prognostically simulates N_2 fixation, water column denitrification, and sedimentary denitrification to quantify the dynamic response of marine nitrogen cycle to idealized atmospheric N deposition and its impact on marine productivity and ODZs.

2. Model Description

We use a Kiel version [*Somes and Oschlies*, 2015] of the UVic Earth System Climate Model [*Weaver et al.*, 2001] to perform the atmospheric N deposition simulations.

2.1. Physical Model

The physical ocean-atmosphere-sea ice model includes a three-dimensional ($1.8 \times 3.6°$, 19 vertical levels) general circulation model of the ocean (Modular Ocean Model 2) with parameterizations such as diffusive mixing along and across isopycnals, eddy-induced tracer advection [*Gent and McWilliams*, 1990], computation of tidally induced diapycnal mixing over rough topography [*Simmons et al.*, 2004], anisotropic viscosity [*Large et al.*, 2001] and zonal isopycnal mixing [*Getzlaff and Dietze*, 2013] schemes to better resolve zonal equatorial currents. A two-dimensional, single-level energy-moisture balance atmosphere and a dynamic-thermodynamic sea ice model are used, forced with prescribed monthly climatological winds [*Kalnay et al.*, 1996] and ice sheets [*Peltier*, 2004].

2.2. Marine Ecosystem-Biogeochemical Model

The marine ecosystem-biogeochemical model coupled within the ocean circulation includes two nutrients in the inorganic (nitrate (NO_3) and phosphate (PO_4)) and organic (dissolved organic nitrogen (DON) and dissolved organic phosphorus (DOP)) phases, two phytoplankton (ordinary and N_2-fixing diazotrophs), zooplankton, sinking detritus, as well as dissolved O_2, dissolved inorganic carbon, and $\Delta^{14}C$ (see *Somes and Oschlies* [2015] for a full description). Iron limitation is calculated using surface dissolved iron estimate from the BLING model [*Galbraith et al.*, 2010]. Our model was initialized with temperature, salinity, nitrate, phosphate, and oxygen from World Ocean Atlas [*Garcia et al.*, 2010b] and dissolved inorganic carbon, alkalinity, and $\Delta^{14}C$ from Global Ocean Data Analysis Project [*Key et al.*, 2004] observations and was run to quasi steady state for over 8000 years with preindustrial boundary conditions. Note that atmospheric N deposition was not included in the preindustrial steady state simulation, which is common practice for global biogeochemical models [e.g., see *Cabré et al.*, 2014].

Diazotrophs grow slower than ordinary phytoplankton due to extra energetic demands of N_2 fixation [*Grosskopf and Laroche*, 2012]. However, since they have no N limitation, they can out-compete ordinary phytoplankton in surface waters that are depleted in NO_3 but still contain sufficient P and Fe (i.e., water with low $N^* = NO_3 - 16PO_4$ from denitrification and high iron from atmospheric deposition). Diazotrophs have the ability to consume DOP in the model, which expands their ecological niche in the oligotrophic ocean [*Somes and Oschlies*, 2015]. They will consume NO_3 if it exists at high concentrations ($>5\ mmol\ m^{-3}$), generally consistent with culture experiments [*Mulholland et al.*, 2001]. Given the large range of uncertainty in some parameters for diazotrophs, we have conducted sensitivity experiments in previous studies (e.g., mortality/grazing rate [*Somes et al.*, 2013], Fe limitation [*Somes et al.*, 2010], and DOP uptake/remineralization [*Somes and Oschlies*, 2015]) and chose values (Table S1 in the supporting information) that best reproduce patterns of N_2 fixation measurements [*Luo et al.*, 2012] and biogeochemical indicators of N_2 fixation (e.g., $N^* = NO_3 - 16PO_4$ in Figure 1).

Water column denitrification occurs when dissolved oxygen becomes depleted in poorly ventilated ODZs, nitrate replaces dissolved oxygen as the electron acceptor during organic matter respiration and is reduced to dinitrogen gas. We use a threshold of $3\ mmol\ m^{-3}$ O_2 [*Codispoti and Christensen*, 1985] that sets where respiration of organic matter occurs equally between denitrification and aerobic respiration. Further above (below) this threshold, a greater fraction of aerobic respiration (denitrification) occurs with complete aerobic respiration above $7\ mmol\ m^{-3}$ O_2. In our course resolution model, we implemented parameterizations in the tropics to better resolve equatorial undercurrents that ventilate ODZs [*Large et al.*, 2001; *Getzlaff and Dietze*, 2013]. Although the ODZs are displaced too close to the equator in the Pacific and Atlantic and still exist in the Bay of Bengal which is not observed in nature, the model reproduces the general region and volume of global ODZs as well as water column denitrification rates within observational uncertainties (Table S2), without applying artificial thresholds to reduce denitrification rates that have been used in past model versions [e.g., see *Moore and Doney*, 2007; *Somes et al.*, 2013].

Sedimentary denitrification is simulated according to an empirical transfer function based on organic carbon sinking flux to the sediments and bottom water dissolved oxygen and nitrate [*Bohlen et al.*, 2012], which is a computationally efficient alternative to coupling a full sediment model. Since our coarse resolution model does not fully resolve continental shelves and coastal dynamics, it predicts sedimentary denitrification that is lower than empirical estimates (Table S2). This suggests that our model underestimates not only sedimentary denitrification but also N_2 fixation that would be needed to balance this additional N loss in steady state.

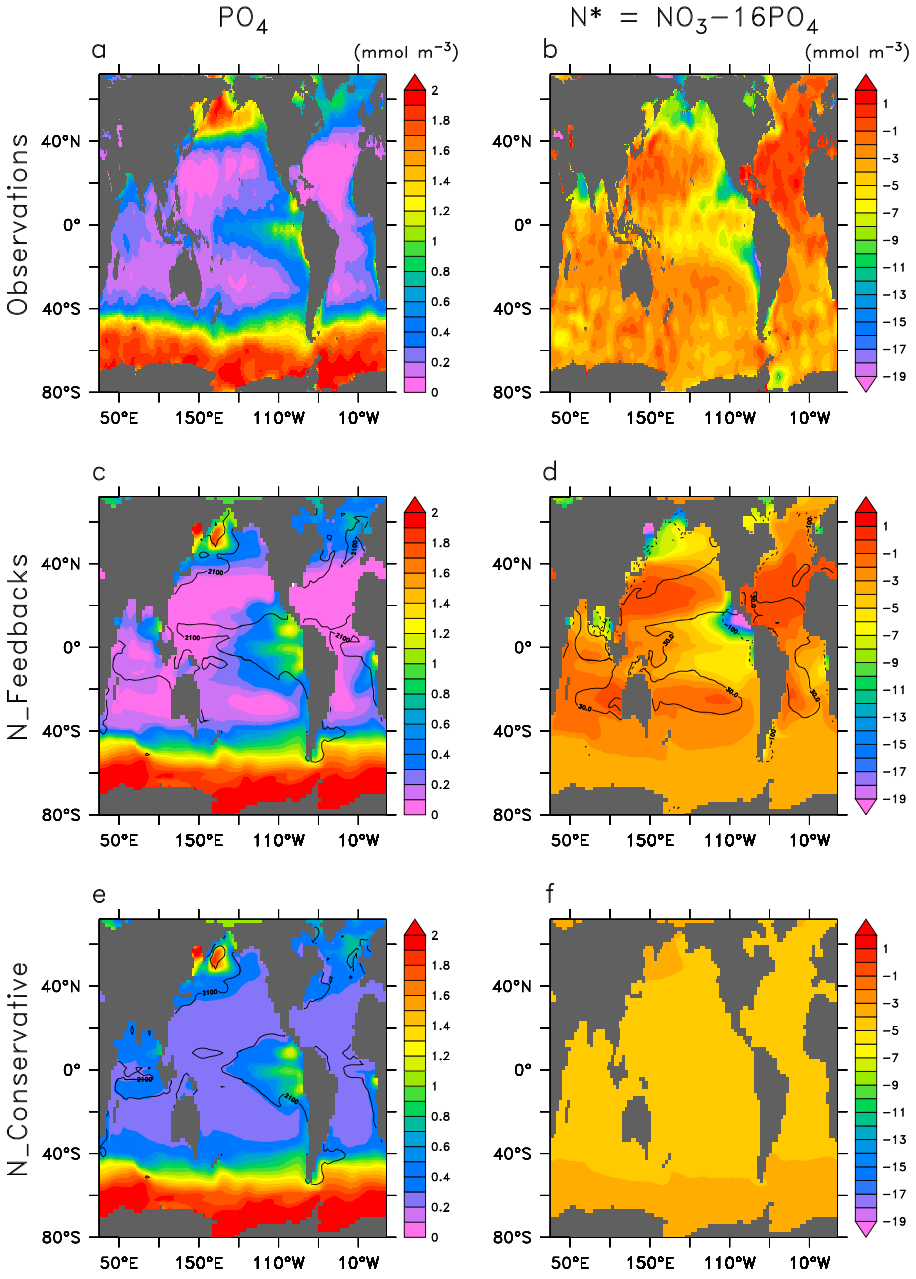

Figure 1. Model-data comparison. Annual comparison of World Ocean Atlas 2009 observations [*Garcia et al.*, 2010a] (a) surface (0–50 m) PO_4 and (b) upper ocean (0–300 m) N* with preindustrial (c, d) N_Feedbacks and (e, f) N_Conservative simulations. Contours of vertically integrated (c, e) net primary production (2100 mmol N m^{-2} yr^{-1}) as well as (d) N_2 fixation (30 mmol N m^{-2} yr^{-1}, lines) and total denitrification (180 mmol N m^{-2} yr^{-1}, dashed lines) are shown.

3. Results

3.1. Local N Addition Simulations

In order to evaluate the spatial and temporal scales of N cycle feedbacks from N_2 fixation and denitrification on the global fixed-N inventory and marine productivity, we performed 689 separate local N addition sensitivity experiments throughout the global ocean. For each simulation, a continuous N addition rate of 50 mmol N m^{-2} yr^{-1}, a moderately high value from the year 2000 observational estimate of atmospheric N deposition [*Duce et al.*, 2008], was applied to NO_3 only in the area of the 2×2 neighboring surface grid boxes ($7.2^o \times 3.6^o$) for 100 years. Due to computational limitations, we performed these experiments only on every

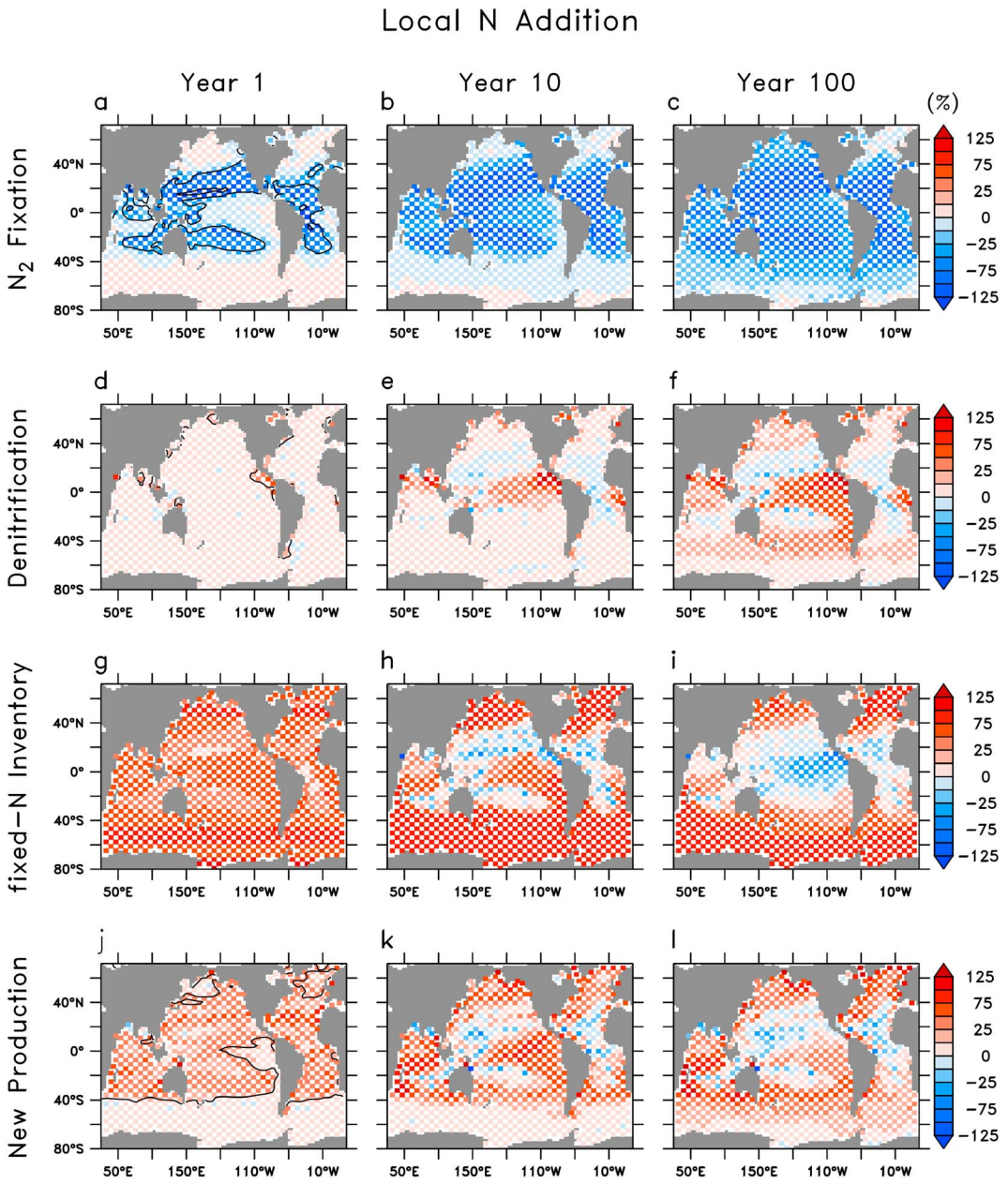

Figure 2. Local N addition simulations. The annual percent changes of (a–c) global N_2 fixation, (d–f) global denitrification, (g–i) global marine fixed-N inventory, and (j–l) global new production (i.e., total net primary production minus euphotic zone remineralization) normalized to the N addition (i.e., [Δ fixed N/N addition] × 100) after 1, 10, and 100 years, respectively. Model experiments were performed on every other set of 2 × 2 grid boxes (colored boxes) and white boxes indicate no experiment at that location. For N_2 fixation, denitrification, and new production, a value of ±100% means this process changed by the exact amount of the N addition rate into the surface ocean grid boxes. For the global fixed-N inventory, the value of 100% means that all of the N addition has accumulated in the ocean, a value of 0% means that there is no net change, and negative values indicate a net loss of global fixed N despite continuous N addition into the respective 2 × 2 surface grid box area. Contours of vertically integrated (a) N_2 fixation (30 and 200 mmol N m^{-2} yr^{-1}) and (d) total denitrification (200 mmol N m^{-2} yr^{-1}), as well as (j) surface NO_3 (3 mmol m^{-3}) are shown from the N_Feedbacks before N addition was applied.

other set of 2 × 2 grid boxes (colored boxes in Figure 2, white boxes indicate locations with no experiment). In Figures 2 and 3, we show the global percent changes of each individual experiment in response to N addition occurring only at the respective location, normalized to the N addition (i.e., [Δ fixed N/N addition] × 100). Figure 3 shows the full transient response in four specific experiments located in the (a) subtropical North Atlantic where N_2 fixation occurs, (b) eastern tropical North Pacific ODZ, (c) North Sea, and (d) Southern Ocean.

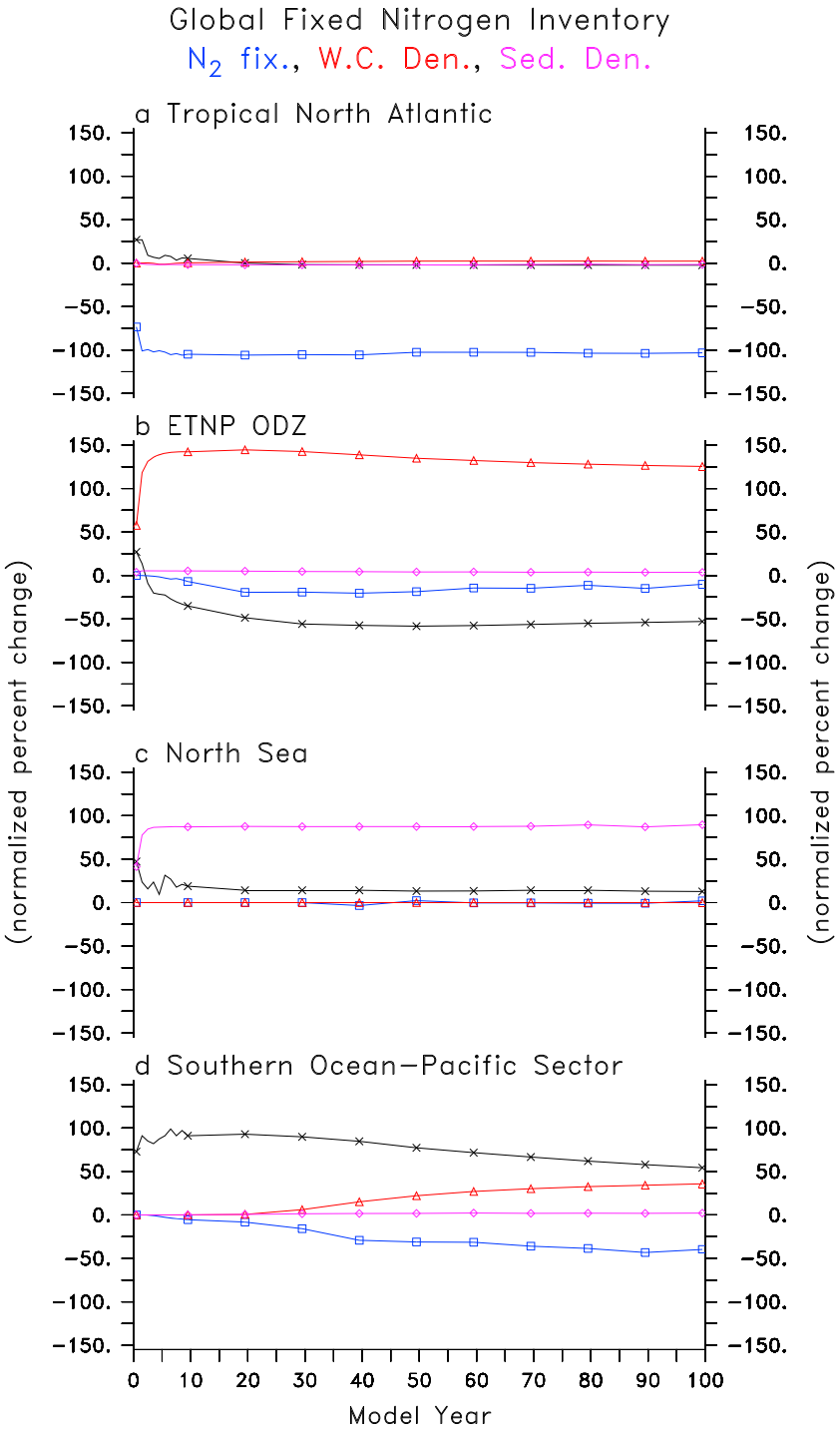

Figure 3. Individual local N addition model results. Transient annual response to N addition on the global marine fixed-N inventory (black asterisks), global N_2 fixation (blue squares), global water column denitrification (red triangles), and global sedimentary denitrification (pink diamonds) shown in percent changes normalized to the N addition rate (consistent with Figure 2 caption) in the (a) Tropical North Atlantic (7.2°N, 39.6°W), (b) Eastern Tropical North Pacific (ETNP) Oxygen Deficient Zone (ODZ) (10.8°N, 90°W), (c) North Sea (55.8°N, 3.6°E), and (d) Pacific sector of the Southern Ocean (43.2°S, 140.4°W).

Upon deposition throughout the tropical/subtropical open ocean where N_2 fixation generally occurs, N_2 fixation decreases nearly instantaneously, which buffers the input from N addition (Figures 2 and 3a). N addition to the surface ocean reduces N limitation and thus diazotrophs' ecological niche in the model. Ordinary phytoplankton then outcompete diazotrophs for available PO_4 in the surface waters due to their higher growth rate [*Hood*, 2004]. Some of the N addition outside regions of N_2 fixation, if not immediately utilized by ordinary phytoplankton, eventually circulates into N_2 fixation regions and drives an additional decrease of N_2 fixation on decadal timescales (Figures 2a–2c).

In regions where N_2 fixation is equal to or higher than local N addition, the reduction in N_2 fixation compensates the N addition and changes to the fixed-N inventory and productivity are small (Figures 2 and 3a). Since the current global anthropogenic N deposition estimate to the oceans (~70 Tg N yr^{-1}) is currently much lower than modern global estimates by the model for N_2 fixation (133 Tg N yr^{-1}), N_2 fixation could, in principle, be able to effectively compensate for much of the global N deposition as long as it reaches regions with N_2 fixation and our assumptions about the sensitivity of the ecological success of diazotrophs to ambient fixed N are correct [*Landolfi et al*., 2015].

Near ODZs where water column denitrification occurs, the local N addition experiments show the counterintuitive result of a net loss to the marine fixed-N inventory (Figures 2h, 2i, and 3b). This is due to denitrification consuming ~7 mol of NO_3 per mol of remineralizing organic nitrogen [*Richards*, 1965]. Therefore, if phytoplankton assimilate all of the N addition into organic matter, which subsequently remineralizes via denitrification in the ODZ, N addition at the surface would generate a hypothesized net N loss cycle [*Landolfi et al*., 2013]. The spatial extent of the net N loss cycle depends on the efficiency by which N addition is assimilated by phytoplankton and remineralized in and around ODZs, which expands with time as N addition continually fuels more organic matter production (Figures 2g–2i).

In our model simulations, the net N loss cycle is most pronounced near the eastern tropical North Pacific ODZ (Figures 2i and 3b) due to strong N limitation in that region, where efficient assimilation of the N addition directly above the ODZ occurs. Higher N_2 fixation exists above the North Indian ODZ due to more iron-replete conditions via atmospheric dust deposition compared to the eastern tropical Pacific. In the Northern Indian Ocean, N_2 fixation decreases in response to N addition and buffers the potential to fuel a strong N loss cycle (Figures 2a–2c). In the more iron-limited and NO_3-replete waters above the eastern tropical South Pacific ODZ, ordinary phytoplankton do not immediately assimilate a large portion of the N addition to cause a strong N loss cycle directly over that ODZ.

N addition at higher latitudes accumulates in the surface open ocean in the model, which can potentially stimulate additional productivity. However, much of the high-latitude ocean is either light or iron limited so N addition still has a limited immediate impact on local marine productivity (e.g., Southern Ocean, Figure 2j). This additional fixed N eventually circulates into the tropics and induces the same stabilizing N cycle feedbacks described above. Since N_2 fixation occurs in closer spatial proximity to the Southern Ocean than denitrification, it responds before denitrification (Figure 3d). The strength and timing of these stabilizing N cycle feedbacks depends on how efficiently the N addition circulates to these locations of N_2 fixation and denitrification, governed by ocean circulation.

On continental shelves, enhanced productivity from N addition increases sedimentary denitrification in the model, which is predicted using an empirical benthic transfer function based on fluxes of organic carbon to the sediments, as well as bottom water oxygen and nitrate [*Bohlen et al*., 2012]. The simulated sedimentary denitrification increase buffers much of the N addition occurring over some continental shelves (e.g., North Sea, Figure 3c). Since only part of the organic matter arrives at the sediment and, depending on bottom water nitrate and oxygen conditions, only part of the sedimentary respiration occurs via denitrification, the sedimentary denitrification feedback is less intense than in water column ODZs and never drives a net benthic N loss cycle according to our model. Nonetheless, enhanced sedimentary denitrification still compensates much of the N addition occurring over the continental shelves.

3.2. Global Atmospheric Nitrogen Deposition Simulations

To better evaluate how these different N cycle feedbacks interact on the global scale, we conducted additional idealized global atmospheric N deposition simulations from empirically estimated patterns and rates

[*Duce et al*., 2008]. These global atmospheric N deposition estimates were applied on two preindustrial model configurations: one including our standard configuration with a prognostic marine nitrogen budget including N_2 fixation, water column denitrification, and sedimentary denitrification (N_Feedbacks, Figures 1 and S4) and another where these processes are removed, and thus, N input via atmospheric deposition will cycle conservatively within the ocean circulation-biogeochemical system (N_Conservative). These two model configurations were chosen to generally reflect the low (N_Conservative) and high (N_Feedbacks) levels of complexity that global climate-biogeochemical models choose to represent marine nitrogen cycling [e.g., see *Cabré et al*., 2015, their Table A3]. Both model versions produce similar large-scale patterns of common biogeochemical variables typically used to validate models such as PO_4 (Figure 1), global net primary production, and ODZ volume (Table S2).

The N_Conservative simulation was achieved by setting diazotroph's growth rate to 0, which eliminates N_2 fixation, and removing the water column and sedimentary denitrification fluxes, while all other parameters remain identical. Thus, it behaves strictly according to the Redfield ratio (N:P = 16) and cannot reproduce observed variations of N* (Figure 1f). The switch to anaerobic respiration via denitrification is also removed, and thus, oxygen can be consumed into negative concentrations in N_Conservative, which occurs in the core of the ODZs. N_Conservative was initialized with the quasi steady state solution from N_Feedbacks and was run for an additional 2500 years as the marine ecosystem-biogeochemical component approached its new steady state with the same global marine fixed-N inventory, iron limitation, and ocean circulation as N_Feedbacks.

In our idealized experiments, we forced both model configurations with an empirical estimate of global N deposition directly from year 2000 (Figure 2a) [*Duce et al*., 2008] for 1000 years, which was applied continuously to the preindustrial quasi steady state solution. Atmospheric CO_2 is prescribed as a constant at preindustrial level, and thus, the seasonally cycling ocean circulation remains unchanged in the atmospheric N deposition perturbation simulations. However, the marine ecosystem-biogeochemical component dynamically reacts to the biogeochemical forcing induced by the extra N input, albeit with the same seasonally cycling iron limitation.

We chose this model setup to focus solely on N cycle feedbacks in response to additional N supply in terms of atmospheric N deposition without the complexities of climate-biogeochemistry interactions. While these simulations have implications for atmospheric nitrogen deposition's contribution to future changes in marine productivity, they should not be interpreted as direct predictions given the idealized nature of these simulations, which do not account for changes to temperature, ocean circulation, and iron cycling. These model perturbation experiments demonstrate the uncertainty associated with different complexities of N cycle model configurations and how they can influence the response of marine productivity to atmospheric N deposition.

The N_Conservative simulation shows a stronger response to the atmospheric N deposition compared to N_Feedbacks (Figures 4 and S2). Fixed N limits productivity throughout much of the tropical/subtropical surface ocean in our model. Therefore, the N deposition input relieves N limitation and stimulates additional productivity (+14.6%) and expansion of the ODZs (+94.6%) after 100 years in N_Conservative (Figure 4), while the changes predicted by N_Feedbacks to marine productivity (+1.8%) and ODZs (+8.6%) are smaller by nearly an order of magnitude. This illustrates that dynamic N cycle feedbacks associated with N_2 fixation and denitrification compensate a substantial part of the atmospheric N deposition in the model.

The strong response in N_Conservative is likely affected by the initial NO_3:PO_4 conditions, which is set to 14.3 according to World Ocean Atlas observations. We chose these initial conditions because it is the most common protocol applied to global ocean biogeochemical models. Since this ratio is lower than the canonical Redfield ratio applied to ordinary phytoplankton (N:P = 16), the model is strongly N limited and sensitive to N input perturbations from atmospheric deposition. The N_Conservative simulation would likely be less sensitive to atmospheric N deposition if the global NO_3:PO_4 was initialized at the Redfield ratio, where the system may shift to P limitation after N input via atmospheric deposition.

In the N_Feedbacks simulation, N_2 fixation and denitrification both act to stabilize the fixed-N inventory and marine productivity in response to global atmospheric N deposition but react on different temporal and spatial scales (Figures 4b and S1). Since N_2 fixation occurs in surface waters that may be directly impacted by deposition, it significantly decreases almost instantaneously to N deposition with 48% of the total decrease

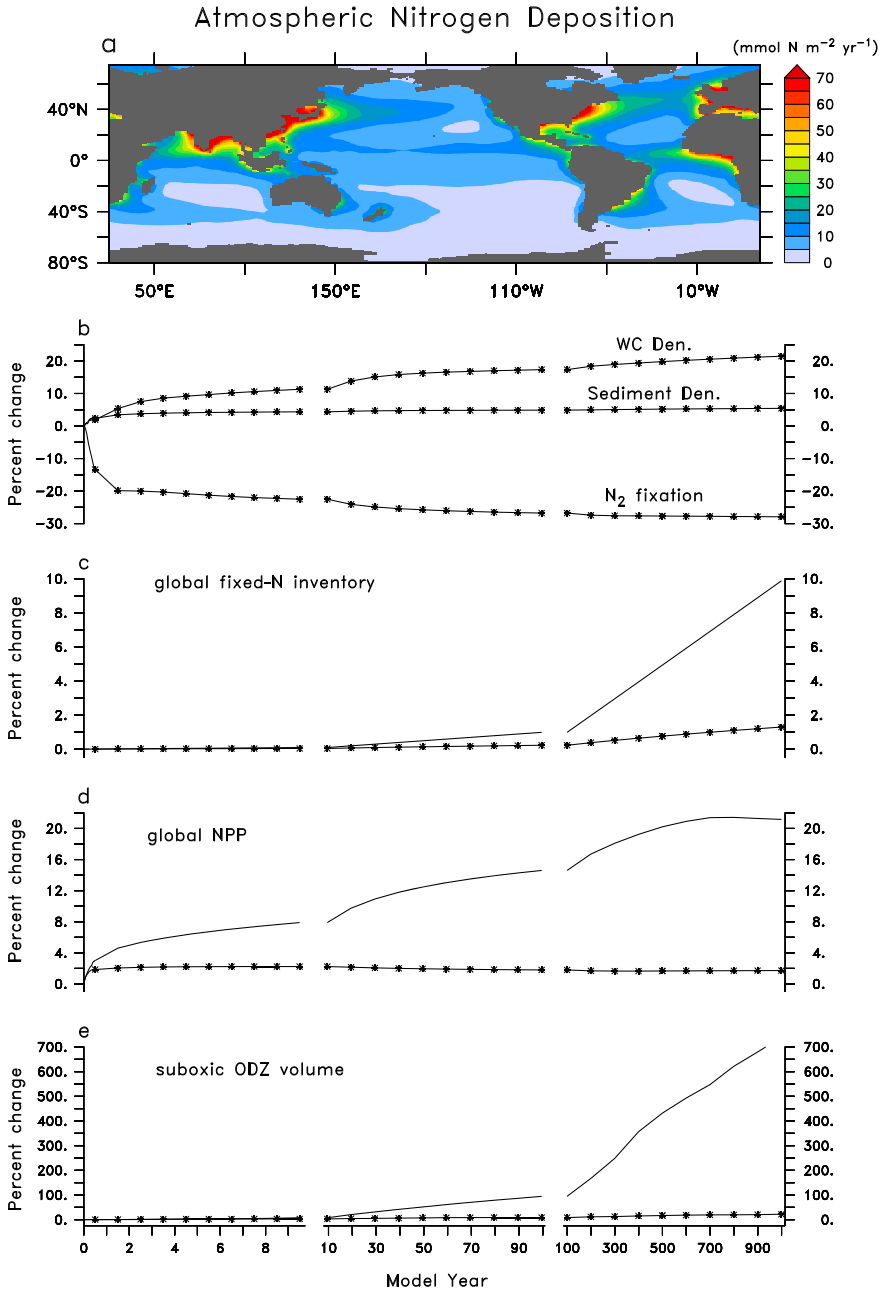

Figure 4. Global atmospheric nitrogen deposition simulations. Comparison of results from N_Feedbacks (i.e., includes N_2 fixation and denitrification; lines with asterisks) and N_Conservative (i.e., excludes N_2 fixation and denitrification; straight lines), in which the (a) year 2000 deposition estimate [*Duce et al.*, 2008] was applied continuously starting at model year 0, of (b) N_2 fixation and denitrification, (c) the global fixed-N inventory, (d) net primary production (NPP), and (e) volume of the suboxic ODZ ($O_2 < 10$ mmol m^{-3}). Percent change is calculated relative to the preindustrial simulations of N_Feedbacks and N_Conservative, respectively, which exclude atmospheric nitrogen deposition.

during the entire millennial simulation occurring within the first year and only another 1.2% decrease between years 100 to 1000. Denitrification shows a more gradual response as it increases by 17% in the first year as well as another 17% between years 100 and 1000.

Atmospheric N deposition occurring in N-limited surface waters stimulates additional organic matter production (Figures 4d and S2i–S2l), most of which is respired aerobically and thereby leads to declining dissolved oxygen levels (Figures 4e and S2q–S2t). However, part of it is respired anaerobically in the slowly expanding

ODZs and thereby increasing denitrification. This denitrification feedback acts as the main buffer to compensate the continuous global N deposition contributing to an increased global fixed-N inventory, marine productivity, and ODZ volume on long timescales in N_Feedbacks compared to N_Conservative (Figure 4).

4. Discussion and Conclusions

Our sensitivity simulation N_Feedback predicts nearly an order of magnitude smaller increase in marine productivity and expansion of ODZs compared to N_Conservative, which excludes feedbacks from N_2 fixation and denitrification (Figures 4d and 4e). In the preindustrial steady state simulation, N_Conservative still produces similar results as N_Feedbacks of many common biogeochemical variables typically used to validate models such as surface PO_4 (Figure 1), global net primary production (Table S2), and volume of ODZs (Table S2). However, it cannot reproduce other tracers more representative of nitrogen cycling such as N* (Figure 1) because biogeochemical cycling in N_Conservative operates at constant stoichiometry according to the Redfield ratio (N:P = 16). This suggests that nitrogen cycling in N_Feebacks is more realistic then N_Conservative. These idealized simulations demonstrate that the level of N cycle complexity included in models can significantly influence the impact of atmospheric N deposition, which should be considered in future predictions of marine productivity.

These simulations highlight the importance of accounting for non-Redfield processes in marine biogeochemical models when evaluating changes to marine N cycling. Our current model includes the major processes that alter dissolved nitrogen to phosphorus ratios (i.e., N_2 fixation, denitrification, dissolved organic phosphorus preferential remineralization, and consumption) [*Somes and Oschlies*, 2015]. However, our model still operates at the Redfield ratio for ordinary phytoplankton and sinking particulate organic matter, which also deviates from Redfield stoichiometry in nature [e.g., *Martiny et al*., 2013], although to a lesser extent than the dissolved ratios, and has been suggested to influence N cycle feedbacks [*Mills and Arrigo*, 2010]. Future model versions should test the importance of other non-Redfield dynamics from plankton in response to atmospheric N deposition that are not included here.

Our modeling results suggest that oceanic feedbacks associated with N_2 fixation and denitrification limit the impact of atmospheric N deposition on marine productivity. We have identified different spatial and temporal scales of N cycle feedbacks on the marine fixed-N inventory in response to atmospheric nitrogen deposition according to our simulations. N_2 fixation provides an immediate stabilizing feedback by declining nearly instantaneously to N deposition. Denitrification, in addition, provides a more slowly operating stabilizing feedback with continuously increasing N loss rates caused by additional remineralization of organic matter stimulated by N deposition near the slowly expanding ODZs. Since our simulated preindustrial rates of benthic denitrification and N_2 fixation are lower than most estimates (Table S2), the strength of their stabilizing N cycle feedbacks may be underestimated in our model.

The water column denitrification feedback causes a net loss of marine fixed N in ODZs in response to atmospheric nitrogen deposition in our model, which occurs due to its stoichiometry of consuming ~7 mol inorganic nitrogen for each mol of remineralizing organic nitrogen produced from deposition. This counterintuitive net fixed-N loss effect [*Landolfi et al*., 2013] makes water column denitrification a globally important nitrogen limiting feedback, despite the small size of ODZs in the global ocean. Our study emphasizes the importance of an adequate representation of the patterns and rates of N_2 fixation, water column denitrification, and sedimentary denitrification to correctly predict the response of marine productivity to atmospheric N deposition and the future evolution of the global marine N cycle.

Acknowledgments

We acknowledge support by Robert Duce (rduce@ocean.tamu.edu) and the projects that synthesized the observational atmospheric nitrogen deposition estimate: Surface Ocean-Lower Atmosphere Study (SOLAS; www.solas-int.org), International Nitrogen Initiative (www.initrogen.org) of SCOPE, the International Geosphere-Biosphere Program (IGBP; www.igbp.kva.se), and the Joint Group of Experts on Scientific Aspects of Marine Environmental Protection (GESAMP; www.gesamp.org). Two anonymous reviewers provided constructive comments that improved the manuscript. C.J. S, W.K., and A.O. were supported by the Deutsche Forschungsgemeinschaft via the Sonderforschungbereich 754 "Climate-Biogeochemistry Interactions in the Tropical Ocean." A.L. was funded by the DFG LA2919/1-1 and BMBF-SOPRAN projects.

References

Bohlen, L., A. W. Dale, and K. Wallmann (2012), Simple transfer functions for calculating benthic fixed nitrogen losses and C:N:P regeneration ratios in global biogeochemical models, *Global Biogeochem. Cycles*, *26*, GB3029, doi:10.1029/2011GB004198.

Cabré, A., I. Marinov, and S. Leung (2014), Consistent global responses of marine ecosystems to future climate change across the IPCC AR5 earth system models, *Clim. Dyn.*, *45*(5–6), 1253–1280, doi:10.1007/s00382-014-2374-3.

Cabré, A., I. Marinov, R. Bernardello, and D. Bianchi (2015), Oxygen minimum zones in the tropical Pacific across CMIP5 models: Mean state differences and climate change trends, *Biogeosciences*, *12*(18), 5429–5454, doi:10.5194/bg-12-5429-2015.

Codispoti, L. A., and J. P. Christensen (1985), Nitrification, denitrification and nitrous oxide cycling in the eastern tropical South Pacific Ocean, *Mar. Chem.*, *16*(4), 277–300.

Duce, R. A., et al. (2008), Impacts of atmospheric anthropogenic nitrogen on the open ocean, *Science*, *320*(5878), 893–897, doi:10.1126/science.1150369.

Galbraith, E. D., A. Gnanadesikan, J. P. Dunne, and M. R. Hiscock (2010), Regional impacts of iron-light colimitation in a global biogeochemical model, *Biogeosciences*, *7*(3), 1043–1064, doi:10.5194/bg-7-1043-2010.

Garcia, H. E., R. A. Locarnini, T. P. Boyer, J. I. Antonov, M. M. Zweng, O. K. Baranov, and D. R. Johnson (2010a), World Ocean Atlas 2009, Volume 4: Nutrients (phosphate, nitrate, silicate), in *NOAA Atlas NESDIS 71*, edited by S. Levitus, 398 pp., U.S. Gov. Print. Off., Washington, D. C.

Garcia, H. E., R. A. Locarnini, T. P. Boyer, J. I. Antonov, O. K. Baranov, M. M. Zweng, and D. R. Johnson (2010b), World Ocean Atlas 2009, Volume 3: Dissolved oxygen, apparent oxygen utilization, and oxygen saturation, in *NOAA Atlas NESDIS 70*, edited by S. Levitus, 344 pp., U.S. Gov. Print. Off., Washington, D. C.

Gent, P. R., and J. C. McWilliams (1990), Isopycnal mixing in ocean circulation models, *J. Phys. Oceanogr.*, *20*(1), 150–155, doi:10.1175/1520-0485(1990)020<0150:IMIOCM>2.0.CO;2.

Getzlaff, J., and H. Dietze (2013), Effects of increased isopycnal diffusivity mimicking the unresolved equatorial intermediate current system in an earth system climate model, *Geophys. Res. Lett.*, *40*, 2166–2170, doi:10.1002/grl.50419.

Grosskopf, T., and J. Laroche (2012), Direct and indirect costs of dinitrogen fixation in Crocosphaera watsonii WH8501 and possible implications for the nitrogen cycle, *Front. Microbiol.*, *3*, 236, doi:10.3389/fmicb.2012.00236.

Gruber, N. (2008), The marine nitrogen cycle: Overview and challenges, in *Nitrogen in the Marine Environment*, 2nd ed., edited by D. G. Capone et al., chap. 1, pp. 1–50, Academic Press, San Diego, Calif.

Hood, R. R. (2004), Modeling the distribution of Trichodesmium and nitrogen fixation in the Atlantic Ocean, *J. Geophys. Res.*, *109*, C06006, doi:10.1029/2002JC001753.

Kalnay, E., et al. (1996), The NCEP/NCAR 40-year reanalysis project, *Bull. Am. Meteorol. Soc.*, *77*(3), 437–471, doi:10.1175/1520-0477(1996)077<0437:tnyrp>2.0.co;2.

Key, R. M., A. Kozyr, C. L. Sabine, K. Lee, R. Wanninkhof, J. L. Bullister, R. A. Feely, F. J. Millero, C. Mordy, and T. H. Peng (2004), A global ocean carbon climatology: Results from Global Data Analysis Project (GLODAP), *Global Biogeochem. Cycles*, *18*, GB4031, doi:10.1029/2004GB002247.

Kim, I. N., K. Lee, N. Gruber, D. M. Karl, J. L. Bullister, S. Yang, and T. W. Kim (2014), Increasing anthropogenic nitrogen in the North Pacific Ocean, *Science*, *346*(6213), 1102–1106, doi:10.1126/science.1258396.

Krishnamurthy, A., J. K. Moore, N. Mahowald, C. Luo, S. C. Doney, K. Lindsay, and C. S. Zender (2009), Impacts of increasing anthropogenic soluble iron and nitrogen deposition on ocean biogeochemistry, *Global Biogeochem. Cycles*, *23*, GB3016, doi:10.1029/2008GB003440.

Landolfi, A., H. Dietze, W. Koeve, and A. Oschlies (2013), Overlooked runaway feedback in the marine nitrogen cycle: The vicious cycle, *Biogeosciences*, *10*(3), 1351–1363, doi:10.5194/bg-10-1351-2013.

Landolfi, A., W. Koeve, H. Dietze, P. Kähler, and A. Oschlies (2015), A new perspective on environmental controls of marine nitrogen fixation, *Geophys. Res. Lett.*, *42*, 4482–4489, doi:10.1002/2015GL063756.

Large, W. G., G. Danabasoglu, J. C. McWilliams, P. R. Gent, and F. O. Bryan (2001), Equatorial circulation of a global ocean climate model with anisotropic horizontal viscosity, *J. Phys. Oceanogr.*, *31*(2), 518–536, doi:10.1175/1520-0485(2001)031<0518:ECOAGO>2.0.CO;2.

Luo, Y. W., et al. (2012), Database of diazotrophs in global ocean: Abundance, biomass and nitrogen fixation rates, *Earth Syst. Sci. Data*, *4*(1), 47–73, doi:10.5194/essd-4-47-2012.

Martiny, A. C., C. T. A. Pham, F. W. Primeau, J. A. Vrugt, J. K. Moore, S. A. Levin, and M. W. Lomas (2013), Strong latitudinal patterns in the elemental ratios of marine plankton and organic matter, *Nat. Geosci.*, *6*(4), 279–283, doi:10.1038/ngeo1757.

Mills, M. M., and K. R. Arrigo (2010), Magnitude of oceanic nitrogen fixation influenced by the nutrient uptake ratio of phytoplankton, *Nat. Geosci.*, *3*(6), 412–416, doi:10.1038/ngeo856.

Moore, J. K., and S. C. Doney (2007), Iron availability limits the ocean nitrogen inventory stabilizing feedbacks between marine denitrification and nitrogen fixation, *Global Biogeochem. Cycles*, *21*, GB2001, doi:10.1029/2006GB002762.

Mulholland, M. R., K. Ohki, and D. G. Capone (2001), Nutrient controls on nitrogen uptake and metabolism by natural populations and cultures of Trichodesmium (Cyanobacteria), *J. Phycol.*, *37*(6), 1001–1009, doi:10.1046/j.1529-8817.2001.00080.x.

Peltier, W. R. (2004), Global glacial isostacy and the surface of the ice-age Earth: The ICE-5G (VM2) model and GRACE, *Annu. Rev. Earth Planet. Sci.*, *32*(1), 111–149, doi:10.1146/annurev.earth.32.082503.144359.

Richards, F. A. (1965), Anoxic basins and fjords, in *Chemical Oceanograpy*, edited by J. P. Riley and G. Skirrow, pp. 611–645, Academic Press, London.

Simmons, H. L., S. R. Jayne, L. C. S. Laurent, and A. J. Weaver (2004), Tidally driven mixing in a numerical model of the ocean general circulation, *Ocean Modell.*, *6*(3-4), 245–263, doi:10.1016/S1463-5003(03)00011-8.

Somes, C. J., and A. Oschlies (2015), On the influence of "non-Redfield" dissolved organic nutrient dynamics on the spatial distribution of N_2 fixation and the size of the marine fixed nitrogen inventory, *Global Biogeochem. Cycles*, *29*, 973–993, doi:10.1002/2014GB005050.

Somes, C. J., A. Schmittner, and M. A. Altabet (2010), Nitrogen isotope simulations show the importance of atmospheric iron deposition for nitrogen fixation across the Pacific Ocean, *Geophys. Res. Lett.*, *37*, L23605, doi:10.1029/2010GL044537.

Somes, C. J., A. Oschlies, and A. Schmittner (2013), Isotopic constraints on the pre-industrial oceanic nitrogen budget, *Biogeosciences*, *10*(9), 5889–5910, doi:10.5194/bg-10-5889-2013.

Weaver, A. J., et al. (2001), The UVic Earth System Climate Model: Model description, climatology, and applications to past, present and future climates, *Atmos. Ocean*, *39*(4), 361–428.